Modification of biochar properties using CO_2

Youkwan Kim[a,1], Jeong-Ik Oh[b,1], Meththika Vithanage[c], Young-Kwon Park[d], Jechan Lee[e], Eilhann E. Kwon[a,*]

[a] Department of Environment and Energy, Sejong University, Seoul 05006, Republic of Korea
[b] Advanced Technology Department, Land & Housing Institute, Daejeon 34047, Republic of Korea
[c] Ecosphere Resilience Research Center, Faculty of Applied Sciences, University of Sri Jayewardenepura, Nugegoda 10250, Sri Lanka
[d] School of Environmental Engineering, University of Seoul, Seoul 02504, Republic of Korea
[e] Department of Environmental and Safety Engineering, Ajou University, Suwon 16499, Republic of Korea

HIGHLIGHTS

- CO_2 helps to modify properties of biochar made via pyrolysis.
- Porosity of biochar can be improved when CO_2 is used in the pyrolysis.
- The modification approach can be applied to precisely engineer biochar for various applications.

ARTICLE INFO

ABSTRACT

Biochar is widely used for various environmental remediation strategies such as soil amendment because of its intrinsic carbon negativity and porosity. Biochar is a charcoal-like material produced via pyrolysis of biomass. To determine an effective method for modification of the porosity and morphology of biochar and establishment of a more sustainable pyrolysis platform for biomass valorization, this study used CO_2 as a reactive gas medium in the biomass pyrolysis process. This study placed emphasis on elucidating the role of CO_2 in the production of biochar from different types of biomass, such as cellulose, xylan, lignin, grass, and oak wood. The surface area and porosity of biochar were strongly related to the type of biomass. Under comparable pyrolysis conditions, the surface area of biochar decreased in the following order: cellulose > xylan > lignin ~ oak wood > grass. The use of CO_2 as the gas medium in biomass pyrolysis affected the surface area and porosity of biochar samples derived from biomass feedstock. For instance, the surface area and total pore volume of the oak-wood-derived biochar produced in the CO_2 environment were twice those produced in the N_2 environment. Given that the increases in the biochar surface area and porosity were attributed to the enhanced release of volatile organic compounds (VOCs) from biomass, CO_2 may have enhanced VOC release (removal) during pyrolysis. Therefore, the use of CO_2 in a pyrolysis platform is expected to be a strategic approach for biomass valorization.

1. Introduction

Global carbon emissions from the combustion of fossil fuels have been regarded as one of the main contributors to global warming in that the additional carbon inputs from this combustion are rapidly surpassing the planet's full capacity to assimilate carbons via the natural carbon cycle [1]. It is noteworthy that carbon inputs from fossil fuel combustion reached up to ~37 Gt in 2018 [2]. Accordingly, reduction of the global consumption of fossil fuels is a strategic and practical approach for alleviating the detrimental (environmental) impacts of

global warming [3]. Over the last two decades, a great deal of research has been conducted on renewable energies in an effort to minimize fossil fuel consumption, and unprecedented advances have been made in this research field [4–6]. Among the various available renewable energies, biofuels, i.e., biogas, bioethanol, and biodiesel, have drawn considerable attention because they are the only carbon-based forms of energy [7–9]. Accordingly, biofuels have been readily implemented and commercialized as alternatives to fossil fuels because of their high compatibility with the present energy infrastructure [10]. Specifically, biofuels are being used in a simple manner, i.e., by being blended with

fossil fuels, which provides great opportunities for these two forms of energy to share existing energy distribution networks [11].

The concept of biorefinery for the production of chemicals from carbon-neutral resources (biomass) has also drawn considerable attention as a strategic approach for mitigating global carbon emissions [12,13]. Among the various available technical (biological, chemical, and thermochemical) pathways for biorefinery, the thermochemical pathway (e.g., pyrolysis and gasification processes) can be a viable technical platform for biomass valorization in that biomass is fully functionalized through long-term evolution to adapt to diverse environments [12,14–16]. Such a functionalized structural matrix of biomass deteriorates the overall efficiency of the biorefinery process [16]. On the basis of these rationales, we can consider biorefinery using a thermochemical platform to be a technically viable option because thermochemical processes are less sensitive to the type of biomass and more suitable for mass production [16]. Pyrolysis is defined as *the thermolysis of a carbonaceous material in an oxygen-free environment*; in this process, carbons in carbon substrates are re-allocated into three pyrogenic products: syngas, pyrolytic oil, and (bio)char [17]. Given that all these pyrogenic products are flammable, they can be directly used as biofuels [17,18]. Moreover, the gaseous and liquid pyrogenic products, i.e., syngas and pyrolytic oil, respectively, can be utilized as effective feedstock for biorefinery [19]. It should be noted that syngas is chemically reactive [20].

Recently, biochar has gained considerable attention because of its carbon negativity, which is attributed to its recalcitrant physicochemical properties [21]. Biochar remains in soil for extremely long periods without any degradation, and it can therefore sequester carbon in soils for such long periods [22]. Thus, biochar has been extensively used in various environmental applications (e.g., soil amendment and environmental remediation) [22]. Numerous studies have been conducted to modify the surface morphology of biochar by various approaches, e.g., control of the operational parameters, use of a reactive gas medium such as steam, and utilization of a catalyst in the pyrolysis process [23]. Given that biochar is a pyrogenic byproduct of the pyrolysis process, modification of the surface morphology of biochar must be considered at the overall process level [24]. In short, it is desirable to develop an effective method to modify all pyrogenic products through a simple unit process for biomass pyrolysis.

In an effort to satisfy the aforementioned technical requirements with the eventual aim of establishment of a more sustainable pyrolysis platform, the present study used CO_2 as a reactive gas medium in biomass pyrolysis. N_2 is commonly used to simulate oxygen-free conditions [25]. Thus, this study placed great emphasis on elucidating the mechanistic role of CO_2 in the thermolysis of biomass. The thermolytic behaviors of various types of biomass (i.e., cellulose, xylan, lignin, grass, and lignocellulosic biomass) in a CO_2 environment in comparison to those in a N_2 environment as reference were characterized thermogravimetrically. Moreover, laboratory-scale pyrolysis of the five types of biomass was performed by controlling the heating rates in the N_2 and CO_2 environments in order to achieve morphological modifications of biochar in CO_2 as the reactive gas medium.

2. Materials and methods

2.1. Sample preparation and chemical agents

Cellulose (product #310697) and lignin (product #370959) were purchased from Sigma-Aldrich (St. Louis, MO, USA). Xylan extracted from corncob (product #X0078) was purchased from Tokyo Chemical Industry (Japan). Grass was collected from Grand Children's Park (37.547691, 127.074234) in Seoul, Republic of Korea. Lignocellulosic biomass (oak wood) was sourced from the Rural Development Administration, Republic of Korea. Grass and lignocellulosic biomass were dried in a drying oven (Ecocell 55, Revodix, Republic of Korea) at 80 °C for 24 h. The size of biomass samples was adjusted to ≤150 μm by

using a ball mill. Ultra-high-purity N_2 and ultra-high-purity CO_2 were purchased from Kukje Industrial Gases (Anyang, Republic of Korea).

2.2. Thermogravimetric analysis of biomass

Mass decay of biomass as a function of the thermolytic temperature was monitored using a thermogravimetric analysis (TGA) unit (STA 449 F5 Jupiter, Netzsch, Germany). For the TGA tests, 10 ± 0.01 mg of biomass was loaded into the TGA unit. The TGA tests was performed at a heating rate of 10 °C min^{-1} in the range of 40–900 °C. The flow rate of N_2 or CO_2 was controlled using mass flow controllers (MFCs) incorporated into the TGA unit. The total flow rate was 70 mL min^{-1} (protective gas: 20 mL min^{-1}; purge gas: 50 mL min^{-1}). Prior to each TGA test, a reference TGA test was performed without sample loading to compensate for any mass change induced by buoyancy effects. These buoyancy effects were attributed to the density variation of N_2 or CO_2 by thermal expansion during the TGA test.

2.3. Laboratory-scale pyrolysis of biomass in CO_2 environment using batch-type tubular reactor

Prior to laboratory-scale pyrolysis of biomass, a batch-type tubular reactor (TR) was assembled, as described in Fig. S1 (Supporting information). To prevent catalytic effects, quartz tubing (CGQ-0800T-68, Chemglass) was employed as the main body of the TR; the dimensions of the TR were 23 mm (inner diameter) × 25.4 mm (outer diameter) × 0.6 m (length). To tap the gas inlet and outlet systems, two stainless Ultra-Torr Vacuum Fittings (SS-4-UT-6-600, Swagelok, USA) were connected to each end of the TR. Furthermore, a Swagelok reducing union (1–0.25 in) was connected to the stainless Ultra-Torr Vacuum Fitting. Biomass (1 ± 0.001 g) was loaded at the center of the TR. The flow rate of N_2 or CO_2 was set as 800 mL min^{-1}; it was controlled using the MFCs (5850 series E, Brooks Instruments, USA). A tubular furnace (RD 30/200/11, Nabertherm, Germany) was used as an external heating source. Prior to gas chromatography (GC) measurements, a cold trap chilled with liquid N_2 was used to collect the carbons in condensable hydrocarbons. Then, pyrolytic gases released from the TR were quantified using an online gas chromatograph (3000A Micro-GC, Inficon, Switzerland). The concentrations of the pyrolytic gases (H_2, CH_4, and CO) were calculated from their respective pre-calibrated plots of peak area versus concentration.

2.4. Quantification, qualification, and characterization of pyrogenic products

The calibration of the gas chromatograph was performed using the natural gas standard (Agilent, USA). A field-emission scanning electron microscope (FE-SEM; S-4300, Hitachi, Japan) equipped with an energy-dispersive X-ray spectrometer was used for morphological and microstructural analyses of the biochar surface. N_2 physisorption was conducted to determine specific surface area, mean pore diameter, and total pore volume of the biochar samples using BELSORP-mini (MicrotracBEL Corp., Osaka, Japan). Non-local density functional theory (NL-DFT) model was used to determine pore size distribution with the assumption of slit-shaped pores.

3. Results and discussion

3.1. Characterization of thermolysis of grass and lignocellulosic biomass (oak wood) in CO_2

A series of TGA tests (biomass: 10 ± 0.01 mg) were performed to characterize the thermolytic behaviors of biomass in a CO_2 environment. The TGA tests of biomass in CO_2 (in comparison to those in N_2 as reference) were performed at a heating rate of 10 °C min^{-1} in the range of 40–900 °C. The mass decay of biomass as a function of the
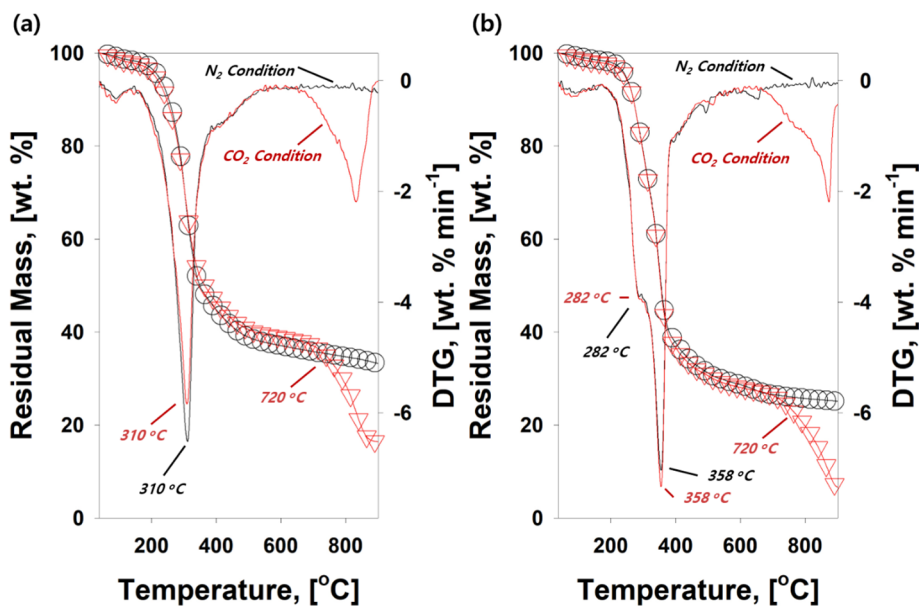
Fig. 1. (a) Mass decay of grass as a function of thermolytic temperature and its thermal degradation rate in N_2 (black) and CO_2 (red) and (b) mass decay of lignocellulosic biomass (oak wood) as a function of thermolytic temperature and its thermal degradation rate in N_2 (black) and CO_2 (red). (For interpretation of the references to colour in this figure legend, the reader is referred to the web version of this article.)
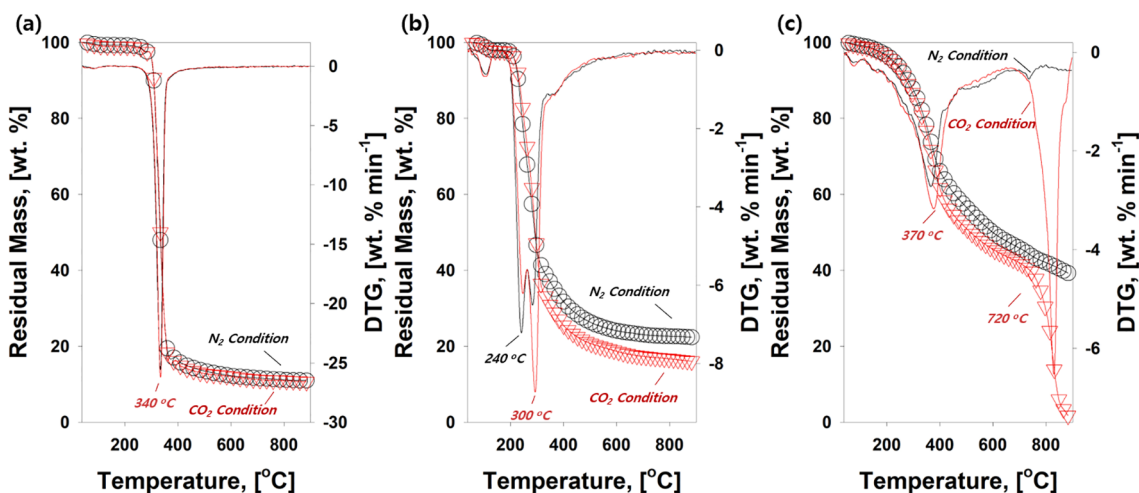

Fig. 2. (a) Mass decay of cellulose as a function of thermolytic temperature and its thermal degradation rate in N_2 (black) and CO_2 (red); (b) mass decay of xylan as a function of thermolytic temperature and its thermal degradation rate in N_2 (black) and CO_2 (red); and (c) mass decay of lignin as a function of thermolytic temperature and its thermal degradation rate in N_2 (black) and CO_2. (For interpretation of the references to colour in this figure legend, the reader is referred to the web version of this article.)

thermolytic temperature is shown in Fig. 1. The thermal degradation rate (differential thermogram (DTG)) is also depicted in this figure to effectively identify any mass decay changes induced by CO_2.

In a typical pyrolysis atmosphere (N_2), there are three distinctive mass decay patterns of grass (Fig. 1(a)). Mass decay first occurs near 100 °C, possibly because of dehydration. Mass decay of grass next occurs at ≤430 °C, at which temperature volatilization occurs; this is followed by random bond scissions of volatile organic compounds (VOCs) from the polymeric backbone of biomass [26]. Thermal degradation occurring at ≥430 °C (i.e., final mass decay) is possibly attributed to dehydrogenation [27]. A difference is observed in the TGA patterns between the N_2 and CO_2 environments at ≥720 °C. More grass is thermally decomposed in the CO_2 environment than in the N_2 environment (final residual mass: ~35 wt% in N_2 and ~15 wt% in CO_2). This is probably a result of the Boudouard reaction (C + CO_2 ⇌ 2CO) [26,27]. It is noteworthy that the Boudouard reaction is thermodynamically favorable at ≥710 °C [28]. Thermolysis of lignocellulosic biomass (oak wood) in N_2 and CO_2 was also characterized thermogravimetrically. As can be seen from Fig. 1(b), the thermolytic

behaviors of lignocellulosic biomass are similar to those of grass (Fig. 1(a)). An interesting observation here is that the final residual mass of grass is higher than that of lignocellulosic biomass.

3.2. Characterization of thermolysis of cellulose, xylan, and lignin in CO_2

The thermolytic behaviors of the main constituents of biomass (cellulose, hemicellulose (xylan), and lignin) were characterized thermogravimetrically in order to gain a fundamental understanding of the mechanistic role of CO_2 in the thermolysis of biomass. It should be noted that all the experimental conditions for the characterization in Fig. 2 were identical to those in Fig. 1. In brief, 10 ± 0.01 mg of cellulose, xylan, or lignin was thermally degraded in N_2 or CO_2 at a heating rate of 10 °C min^{-1} in the range of 40–900 °C.

As can be seen in Fig. 2(a), the mass decay patterns of xylose and lignin in CO_2 are different from those in N_2. Interestingly, at ≤720 °C, larger amounts of xylan and lignin thermally degraded during TGA in CO_2 than in N_2. The identical thermolytic patterns of cellulose in N_2 and CO_2 may be a result of the high mass fraction of volatile matter in
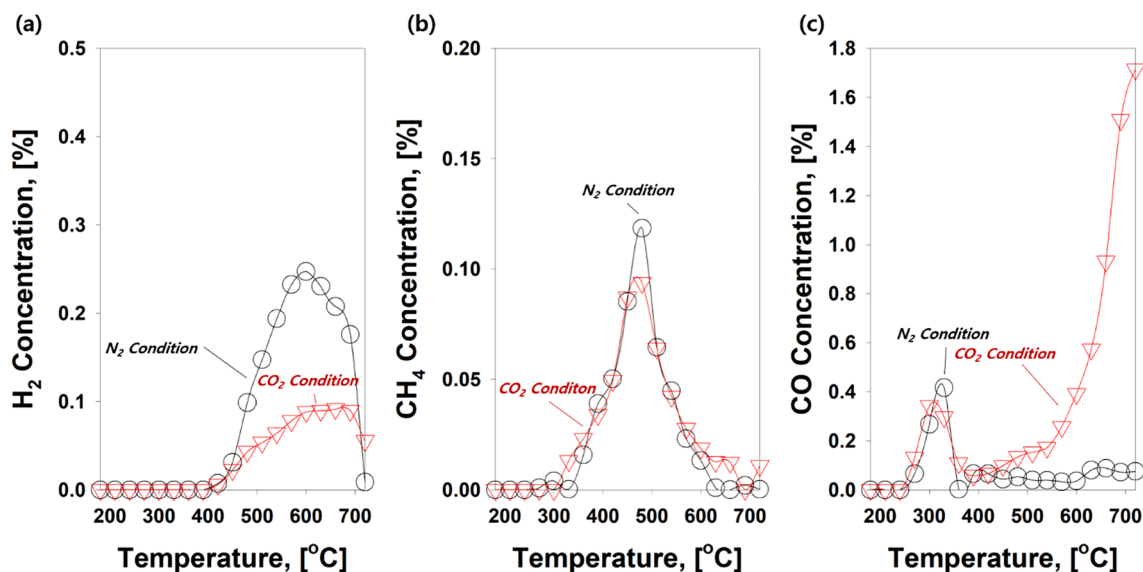
Fig. 3. Concentration profiles of main pyrolytic gases ((a) H_2, (b) CH_4, and (c) CO) evolved from thermolysis of grass (1 $\pm$ 0.01 g) in N_2 and CO_2 environments at a heating rate of 10 °C min^{-1} in the temperature range of 40–720 °C.
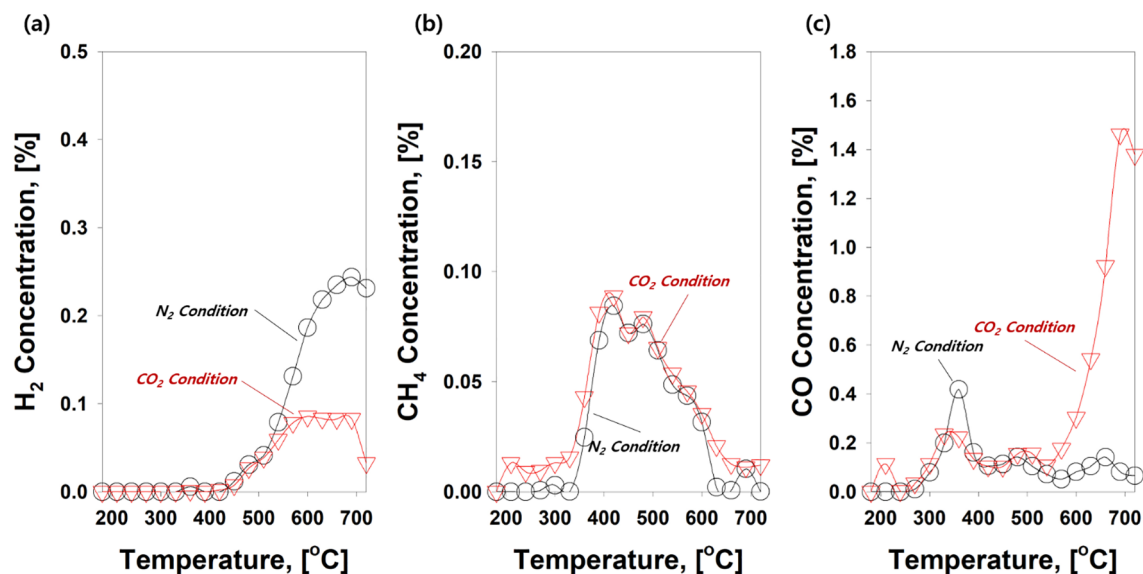

Fig. 4. Concentration profiles of main pyrolytic gases ((a) H_2, (b) CH_4, and (c) CO) evolved from thermolysis of lignocellulosic biomass (oak wood; 1 $\pm$ 0.01 g) in N_2 and CO_2 at a heating rate of 10 °C min^{-1} in the range of 40–720 °C.

cellulose. Fig. 2 shows that the Boudouard reaction occurred only during the thermolysis of lignin. It can be speculated that the occurrence of the Boudouard reaction is highly dependent on the characteristics of biomass (i.e., the raw material of biochar). It has been reported that different constituents of biomass have different sensitivities to CO_2 in the pyrolysis process [29].

3.3. Pyrolysis of biomass in CO_2

The series of TGA tests revealed important implications. Nonetheless, it was desirable to monitor the gas evolution patterns in order to support all hypotheses experimentally. Except the sample loading and the flow rate of N_2 or CO_2, all the experimental conditions were identical to the conditions in the TGA test. In brief, laboratory-scale pyrolysis of biomass (1 $\pm$ 0.001 g) was performed at a heating rate of 10 °C min^{-1} in the range of 40–710 °C. It should be noted that the final temperature for the laboratory-scale pyrolysis was set as 710 °C to exclude any effects of the Boudouard reaction. The

concentration profiles of the main pyrolytic gases (H_2, CH_4, and CO) evolved from the thermolysis of grass in N_2 and CO_2 environments were plotted as a function of the thermolytic temperature, as shown in Fig. 3.

The concentration profile of H_2 evolved from the thermolysis of grass in N_2 is in good agreement with the TGA test results (Fig. 1(a)). As seen in Fig. 3, evolution of H_2 from the thermolysis of grass in N_2 commenced at ≥ 430 °C. As shown in Fig. 1(a), the thermolytic rate of grass began to decrease at ≥ 430 °C. The H_2 evolution pattern is consistent with the typical trend observed during biomass pyrolysis; that is, the degree of dehydrogenation is proportional to the thermolytic temperature [30]. At 620 °C, the concentration of H_2 began to decrease. This behavior is probably a result of depletion of the H_2 source caused by a batch-type experimental setup (see Fig. S1).

In comparison with H_2, CH_4 began to evolve at ≥ 320 °C and attained the maximum concentration (0.13 mol%) at 490 °C. The earlier evolution of CH_4 than of H_2 can be explained by the formation mechanisms of the former. The evolution of CH_4 is attributed to the thermal cracking of hydrocarbons [31]. Given that rapid mass decay
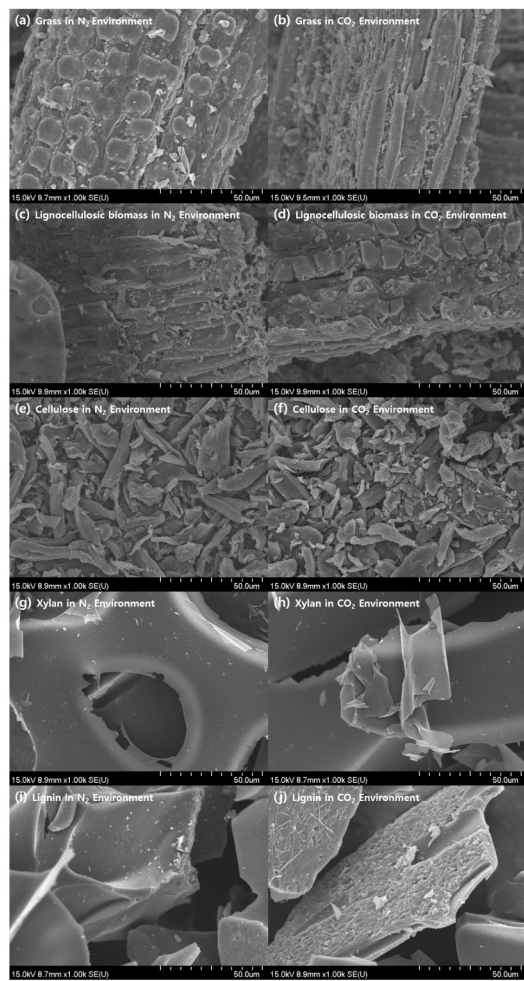
Fig. 5. FE-SEM images of (a), (b) grass biochar produced by pyrolysis in (a) N_2 and (b) CO_2; (c), (d) lignocellulosic biochar produced by pyrolysis in (c) N_2 and (d) CO_2; (e), (f) cellulose biochar produced by pyrolysis in (e) N_2 and (f) CO_2; (g), (h) xylan biochar produced by pyrolysis in (g) N_2 and (h) CO_2; and (i), (j) lignin biochar produced by pyrolysis in (i) N_2 and (j) CO_2. In all cases, pyrolysis of biomass was performed at a heating rate of $10\,°C\,min^{-1}$ in the range of 40–680 °C.

Fig. 6. FE-SEM images of (a), (b) grass biochar produced by pyrolysis in (a) N_2 and (b) CO_2; (c), (d) lignocellulosic biochar produced by pyrolysis in (c) N_2 and (d) CO_2; (e), (f) cellulose biochar produced by pyrolysis in (e) N_2 and (f) CO_2; (g), (h) xylan biochar produced by pyrolysis in (g) N_2 and (h) CO_2; and (i), (j) lignin biochar produced by pyrolysis in (i) N_2 and (j) CO_2. In all cases, pyrolysis of biomass was performed at a heating rate of $50\,°C\,min^{-1}$ in the range of 40–680 °C, after which the biomass sample was isothermally treated for 6 min.

caused by the release of VOCs was observed at $\leq 430\,°C$ in the TGA test of grass (Fig. 1(a)), it is appropriate to conclude that the earlier evolution of CH_4 occurred via the thermal cracking of the VOCs. However, CH_4 formation implies that thermal cracking of VOCs is possible only at $\geq 320\,°C$. After reaching the maximum at 490 °C, the concentration of CH_4 began to decrease because of the depletion of the VOCs in the grass sample. The same explanations are also valid for the evolution of CO. The relatively lower concentration of CO than of H_2 and CH_4 is attributed to the cyclization and carbonization reactions. This observation is also in good agreement with the TGA test results in Fig. 1(a).

However, the concentration of CO evolved from the thermolysis of grass in CO_2 began to increase at $\geq 430\,°C$. It is noteworthy that mass decay caused by the Boudouard reaction was observed at $\geq 720\,°C$ (Fig. 1(a)). On the basis of all these experimental findings, the enhanced formation of CO in the CO_2 environment cannot be explained without consideration of an additional source of C and O. Thus, this enhanced formation of CO during the pyrolysis of grass in the CO_2 environment can be explained by the release of VOCs from biomass during the pyrolysis process. The concentration profiles of CH_4 evolved from the pyrolysis process in N_2 and CO_2 were similar, whereas a larger amount of CO evolved in CO_2 than in N_2. This result also supports the enhanced release of VOCs from the biomass sample during pyrolysis.
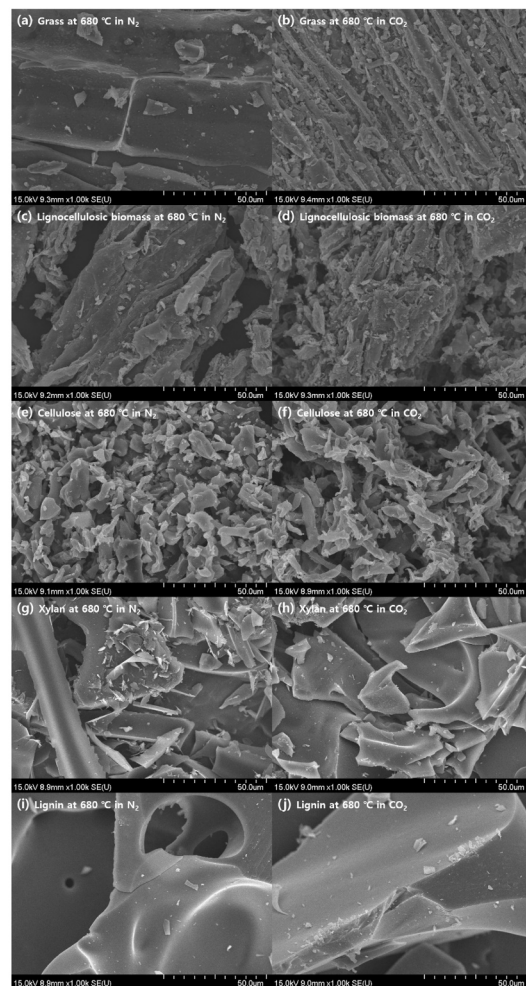
In order to generalize the experimental findings in Fig. 3, we performed the same experiment with lignocellulosic biomass (oak wood) in N_2 and CO_2 environments. As is clear from Fig. 4, the evolution patterns of the main pyrolytic gases in N_2 and CO_2 are identical to those depicted in Fig. 3. Thus, the same explanations provided for the results in Fig. 3 are also valid for the results in Fig. 4. However, in the experiment with lignocellulosic biomass, enhanced CO formation was observed at $\geq 550\,°C$. This observation importantly suggests that the VOC removal from biomass during the pyrolysis process is highly dependent on the structural matrix of biomass.

3.4. Differences in biochar properties arising from use of CO_2 in pyrolysis

In order to experimentally confirm the CO_2-induced morphological modifications of biochar, it was produced at 680 °C. The final temperature of 680 °C was set to exclude any effects of the Boudouard reaction. Given the fact that the heating rate is one of the important operational parameters, biochar was produced by both slow pyrolysis and fast pyrolysis. In detail, slow pyrolysis of biomass was performed at a heating rate of $10\,°C\,min^{-1}$ in the range of 40–680 °C; fast pyrolysis was performed at a heating rate of $50\,°C\,min^{-1}$ in the same temperature range, after which the biomass sample was isothermally treated for

Table 1

Summary of surface area, mean pore diameter, and total pore volume of biochar samples derived from different types of biomass.

Atmospheric condition	Heating rate ($^{\circ}C\,min^{-1}$)	Biochar feedstock	BET surface area ($m^2\,g^{-1}$)	Mean pore diameter (nm)	Total pore volume ($cm^3\,g^{-1}$)
N_2	10	Grass	6.5783	13.839	1.5114
CO_2		Grass	21.253	13.545	4.8829
N_2	50	Grass	11.662	9.329	2.6793
CO_2		Grass	24.674	5.6429	5.6689
N_2	10	Oak wood	231.15	1.9709	53.108
CO_2		Oak wood	463.58	1.9969	106.51
N_2	50	Oak wood	292.99	2.0646	67.316
CO_2		Oak wood	386.76	1.8938	88.860
N_2	10	Cellulose	507.53	1.6679	116.61
CO_2		Cellulose	506.94	1.6643	116.47
N_2	50	Cellulose	504.55	1.6678	115.92
CO_2		Cellulose	515.04	1.6398	118.33
N_2	10	Xylan	340.43	2.0224	78.216
CO_2		Xylan	402.35	1.6324	92.441
N_2	50	Xylan	N.D.	N.D.	N.D.
CO_2		Xylan	N.D.	N.D.	N.D.
N_2	10	Lignin	299.97	1.6624	68.918
CO_2		Lignin	325.85	1.6365	74.865
N_2	50	Lignin	360.31	1.6372	82.782
CO_2		Lignin	402.35	1.6342	92.441

6 min.

The gas evolution patterns in Section 3.3 confirmed that the use of CO_2 as the reactive gas medium led to different thermolytic pathways. We assumed that these different thermolytic pathways resulting from the CO_2 environment induced morphological modifications of biochar. Figs. 5 and 6 show FE-SEM images of biochar samples produced by slow pyrolysis and fast pyrolysis, respectively, of the different types of biomass under different pyrolysis conditions. These FE-SEM images show that these biochar samples have irregular and wrinkled surface morphologies. No clear difference can be observed between these biochar samples. To determine the differences between the biochar samples derived from the different types of biomass in the CO_2 environment, we performed a series of N_2 physisorption measurements (using 20 different biochar samples); Table 1 summarizes the results of all the N_2 physisorption measurements.

Fig. 7 shows the surface area, total pore volume, and mean pore diameter of grass biochar and lignocellulosic (oak wood) biochar, respectively, produced by slow pyrolysis and fast pyrolysis in N_2 and CO_2, and Table 1 lists the corresponding measurement results. It can be seen from Fig. 7 that the surface area and total pore volume of grass biochar produced in the CO_2 environment are higher than those in the N_2 environment. The CO_2-induced morphological modifications of grass biochar during fast pyrolysis (high heating rate of $50\,^{\circ}C\,min^{-1}$) are insignificant compared to those during slow pyrolysis. It is known that the removal of residual VOCs from biochar leads to an increase in the surface area and porosity of biochar [32,33]. Therefore, the CO_2-induced modifications of the biochar properties during the pyrolysis process (depicted in Fig. 7 and summarized in Table 1) are a result of
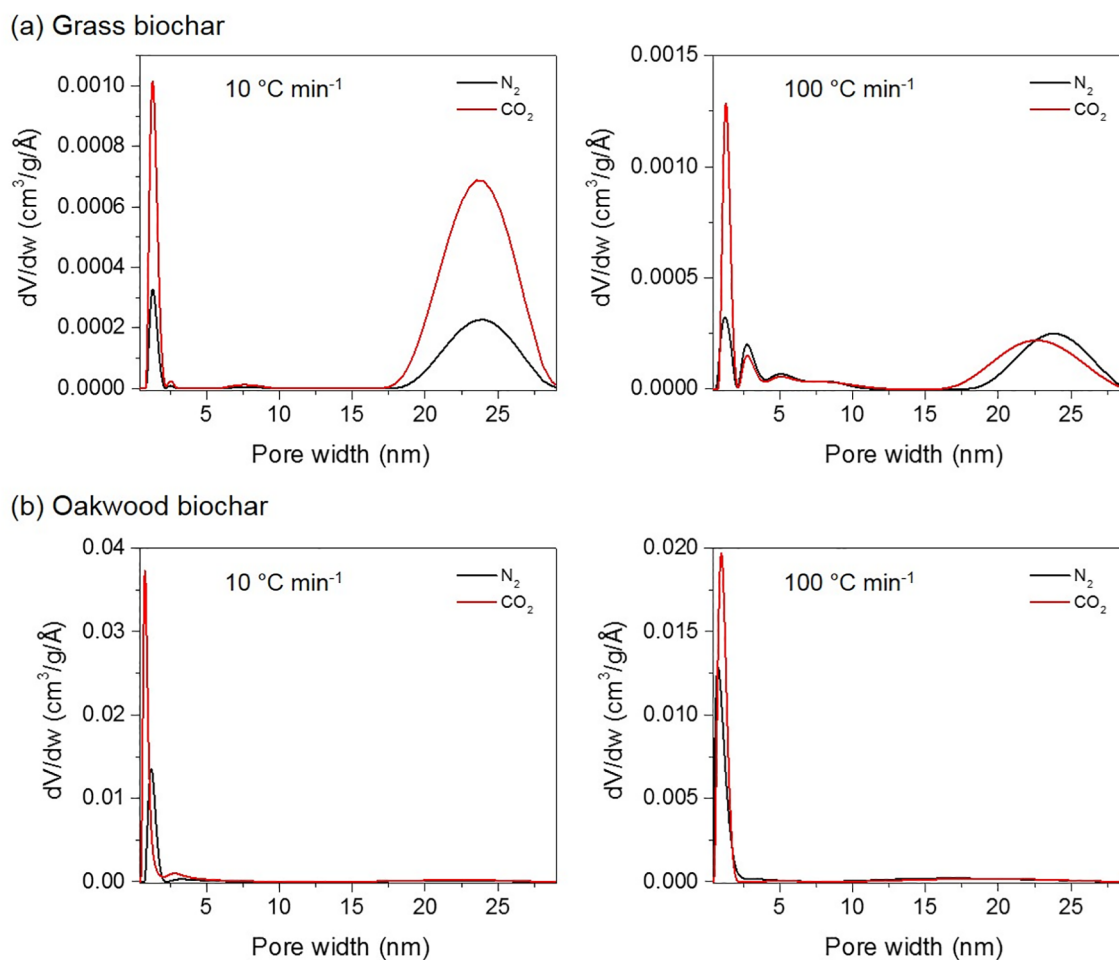

Fig. 7. Pore volume weighted pore size-distribution derived from N_2 physisorption of (a) grass biochar and (b) oakwood biochar made via pyrolysis at different heating rates in N_2 and CO_2.

the enhanced release of VOCs induced by CO_2, as discussed in the above sections. It is pertinent to note that the aforementioned mechanistic role of CO_2 is not fully activated, because of the short thermolysis time (i.e., fast pyrolysis). The N_2 physisorption measurement results of the lignocellulosic (oak wood) biochar produced by slow and fast pyrolysis in N_2 and CO_2 follow the same trends as those of the grass biochar. Thus, the characterization results of the lignocellulosic biochar can be interpreted in the same manner as those of the grass biochar.

4. Conclusions

In this study, CO_2 was used as a gas medium in biomass pyrolysis in order to modify the surface area and porosity of the resultant biochar. Five different types of biomass—cellulose, xylan, lignin, grass, and oak wood—were used as biochar feedstock. Among the tested biochar samples, cellulose biochar showed the highest BET surface area ($> 500\,m^2\,g^{-1}$) whereas grass biochar showed the lowest BET surface area (6.6–24.7 $m^2\,g^{-1}$). The use of CO_2 in the pyrolysis process resulted in an increased surface area and pore volume of biochar. For instance, the BET surface area and total pore volume of the oak-wood-derived biochar produced in the CO_2 environment (463.6 $m^2\,g^{-1}$ and 106.5 $cm^3\,g^{-1}$, respectively) were almost twice those of the oak-wood-derived biochar produced in the N_2 environment (231.2 $m^2\,g^{-1}$ and 53.1 $cm^3\,g^{-1}$, respectively). These differences in the surface areas and porosities of the different biochar samples are possibly attributable to the enhanced release (i.e., removal) of VOCs from the biomass samples caused by CO_2 during the pyrolysis process.

Acknowledgements

Declarations of interest

None.

Appendix A. Supplementary data

Supplementary data to this article can be found online at https://doi.org/10.1016/j.cej.2019.04.170.

References

[1] Z. Liu, Z. Zhang, Z. Jia, L. Zhao, T. Zhang, W. Xing, S. Komarneni, F. Subhan, Z. Yan, New strategy to prepare ultramicroporous carbon by ionic activation for superior CO_2 capture, Chem. Eng. J. 337 (2018) 290–299.

[2] M. Jiang, X. Gao, Q. Guan, X. Hao, F. An, The structural roles of sectors and their contributions to global carbon emissions: a complex network perspective, J. Clean. Prod. 208 (2019) 426–435.

[3] M.V. Rechberger, S. Kloss, H. Rennhofer, J. Tintner, A. Watzinger, G. Soja, H. Lichtenegger, F. Zehetner, Changes in biochar physical and chemical properties: accelerated biochar aging in an acidic soil, Carbon 115 (2017) 209–219.

[4] N.L. Panwar, S.C. Kaushik, S. Kothari, Role of renewable energy sources in environmental protection: a review, Renew. Sustain. Energy Rev. 15 (2011) 1513–1524.

[5] A. Holma, P. Leskinen, T. Myllyviita, K. Manninen, L. Sokka, T. Sinkko, K. Pasanen, Environmental impacts and risks of the national renewable energy targets – a review and a qualitative case study from Finland, Renew. Sustain. Energy Rev. 82 (2018) 1433–1441.

[6] E.J. Novaes Menezes, A.M. Araújo, N.S. Bouchonneau da Silva, A review on wind turbine control and its associated methods, J. Clean. Prod. 174 (2018) 945–953.

[7] M. Parsaee, M. Kiani Deh Kiani, K. Karimi, A review of biogas production from sugarcane vinasse, Biomass Bioenergy 122 (2019) 117–125.

[8] Y. Zhao, A. Damgaard, T.H. Christensen, Bioethanol from corn stover – a review and technical assessment of alternative biotechnologies, Prog. Energy Combust. Sci. 67 (2018) 275–291.

[9] H. Hosseinzadeh-Bandbafha, M. Tabatabaei, M. Aghbashlo, M. Khanali, A. Demirbas, A comprehensive review on the environmental impacts of diesel/biodiesel additives, Energy Convers. Manage. 174 (2018) 579–614.

[10] M. Morales, P. Collet, L. Lardon, A. Hélias, J.-P. Steyer, O. Bernard, Chapter 20 – life-cycle assessment of microalgal-based biofuel, in: A. Pandey, J.-S. Chang, C.R. Soccol, D.-J. Lee, Y. Chisti (Eds.), Biofuels from Algae, second ed., Elsevier, 2019, pp. 507–550.

[11] L. Lardon, A. Hélias, B. Sialve, J.-P. Steyer, O. Bernard, Life-cycle assessment of biodiesel production from microalgae, Environ. Sci. Technol. 43 (2009) 6475–6481.

[12] R.A. Sheldon, The E factor 25 years on: the rise of green chemistry and sustainability, Green Chem. 19 (2017) 18–43.

[13] V.K. Ponnusamy, D.D. Nguyen, J. Dharmaraja, S. Shobana, J.R. Banu, R.G. Saratale, S.W. Chang, G. Kumar, A review on lignin structure, pretreatments, fermentation reactions and biorefinery potential, Bioresour. Technol. 271 (2019) 462–472.

[14] H. Ohara, Biorefinery, Appl. Microbiol. Biotechnol. 62 (2003) 474–477.

[15] Q. Dang, W. Hu, M. Rover, R.C. Brown, M.M. Wright, Economics of biofuels and bioproducts from an integrated pyrolysis biorefinery, Biofuels Bioprod. Biorefin. 10 (2016) 790–803.

[16] J. Zetterholm, K. Pettersson, S. Leduc, S. Mesfun, J. Lundgren, E. Wetterlund, Resource efficiency or economy of scale: biorefinery supply chain configurations for co-gasification of black liquor and pyrolysis liquids, Appl. Energy 230 (2018) 912–924.

[17] T. Kan, V. Strezov, T.J. Evans, Lignocellulosic biomass pyrolysis: A review of product properties and effects of pyrolysis parameters, Renew. Sustain. Energy Rev. 57 (2016) 1126–1140.

[18] S.S. Lam, R.K. Liew, A. Jusoh, C.T. Chong, F.N. Ani, H.A. Chase, Progress in waste oil to sustainable energy, with emphasis on pyrolysis techniques, Renew. Sustain. Energy Rev. 53 (2016) 741–753.

[19] S.-S. Kim, H.V. Ly, J. Kim, E.Y. Lee, H.C. Woo, Pyrolysis of microalgae residual biomass derived from Dunaliella tertiolecta after lipid extraction and carbohydrate saccharification, Chem. Eng. J. 263 (2015) 194–199.

[20] F. Cherubini, The biorefinery concept: using biomass instead of oil for producing energy and chemicals, Energy Convers. Manage. 51 (2010) 1412–1421.

[21] L. Lonappan, Y. Liu, T. Rouissi, F. Pourcel, S.K. Brar, M. Verma, R.Y. Surampalli, Covalent immobilization of laccase on citric acid functionalized micro-biochars derived from different feedstock and removal of diclofenac, Chem. Eng. J. 351 (2018) 985–994.

[22] Y. Yao, B. Gao, J. Fang, M. Zhang, H. Chen, Y. Zhou, A.E. Creamer, Y. Sun, L. Yang, Characterization and environmental applications of clay–biochar composites, Chem. Eng. J. 242 (2014) 136–143.

[23] K. Yoon, D.-W. Cho, Y.F. Tsang, D.C.W. Tsang, E.E. Kwon, H. Song, Synthesis of functionalised biochar using red mud, lignin, and carbon dioxide as raw materials, Chem. Eng. J. 361 (2019) 1597–1604.

[24] S. You, Y.S. Ok, S.S. Chen, D.C.W. Tsang, E.E. Kwon, J. Lee, C.-H. Wang, A critical review on sustainable biochar system through gasification: Energy and environmental applications, Bioresour. Technol. 246 (2017) 242–253.

[25] A. Khan, J.E. Szulejko, P. Samaddar, K.-H. Kim, B. Liu, H.A. Maitlo, X. Yang, Y.S. Ok, The potential of biochar as sorptive media for removal of hazardous benzene in air, Chem. Eng. J. 361 (2019) 1576–1585.

[26] E.E. Kwon, S.-H. Cho, S. Kim, Synergetic sustainability enhancement via utilization of carbon dioxide as carbon neutral chemical feedstock in the thermo-chemical processing of biomass, Environ. Sci. Technol. 49 (2015) 5028–5034.

[27] E.E. Kwon, E.-C. Jeon, M.J. Castaldi, Y.J. Jeon, Effect of carbon dioxide on the thermal degradation of lignocellulosic biomass, Environ. Sci. Technol. 47 (2013) 10541–10547.

[28] E.E. Kwon, S. Kim, J. Lee, Pyrolysis of waste feedstocks in CO_2 for effective energy recovery and waste treatment, J. CO_2 Util. 31 (2019) 173–180.

[29] J. Lee, Y.F. Tsang, J.-I. Oh, S.-R. Lee, E.E. Kwon, Evaluating the susceptibility of pyrolysis of monosaccharide, disaccharide, and polysaccharide to CO_2, Energy Convers. Manage. 138 (2017) 338–345.

[30] E.E. Kwon, M.J. Castaldi, Mechanistic understanding of polycyclic aromatic hydrocarbons (PAHs) from the thermal degradation of tires under various oxygen concentration atmospheres, Environ. Sci. Technol. 46 (2012) 12921–12926.

[31] E. Kwon, M.J. Castaldi, Investigation of mechanisms of polycyclic aromatic hydrocarbons (PAHs) initiated from the thermal degradation of styrene butadiene rubber (SBR) in N_2 atmosphere, Environ. Sci. Technol. 42 (2008) 2175–2180.

[32] E. Antunes, M.V. Jacob, G. Brodie, P.A. Schneider, Silver removal from aqueous solution by biochar produced from biosolids via microwave pyrolysis, J. Environ. Manage. 203 (2017) 264–272.

[33] X. Dong, G. Li, Q. Lin, X. Zhao, Quantity and quality changes of biochar aged for 5 years in soil under field conditions, CATENA 159 (2017) 136–143.